Dual-Energy CTA for GI Bleeding: Reducing Patient Radiation Dose and Table Time

Steven Hang, MD, Jonathan Chahin, MD, A.J. Pesch, MD, James T. Patrie, MS+, Klaus D. Hagspiel, MD
Department of Radiology and Medical Imaging and Department of Public Health Sciences+, University of Virginia, Charlottesville, VA

Purpose:

- Gastrointestinal (GI) bleeding is common in the United States, requiring hospitalization in 223 per 100,000 people each year (Laine 2012).
- In hemodynamically stable patients, our diagnostic workflow in the Emergency Department typically begins with CTA abdomen/pelvis after physical exam. Previously, our CTA protocol for GI bleeding (GIB CTA) included 3 separate acquisitions performed at single-energy: Non-contrast, Arterial, and Delayed Venous images.

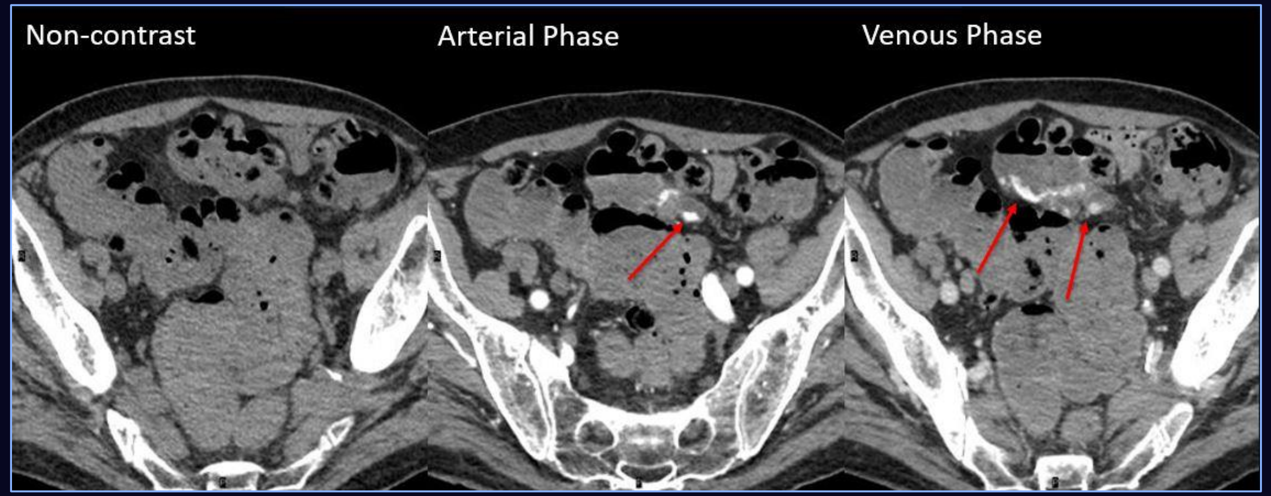

Single-energy GIB CTA demonstrating the development of intraluminal contrast material (red arrows) in the sigmoid colon on the arterial and subsequent venous phase images. This is consistent with active extravasation of contrast representing lower gastrointestinal bleeding.

Effective Dose: 48.6 mSv
Table Time: 4:34 min

- Dual-energy CTA (DE CTA) has been increasingly used in this setting to reduce radiation dose and patient table time because of the ability to create virtual non-contrast (VNC) images and forego the true non-contrast (TNC) acquisition.
- DE CTA also provides potentially clinically useful reconstructions such as iodine maps and virtual monoenergetic images.

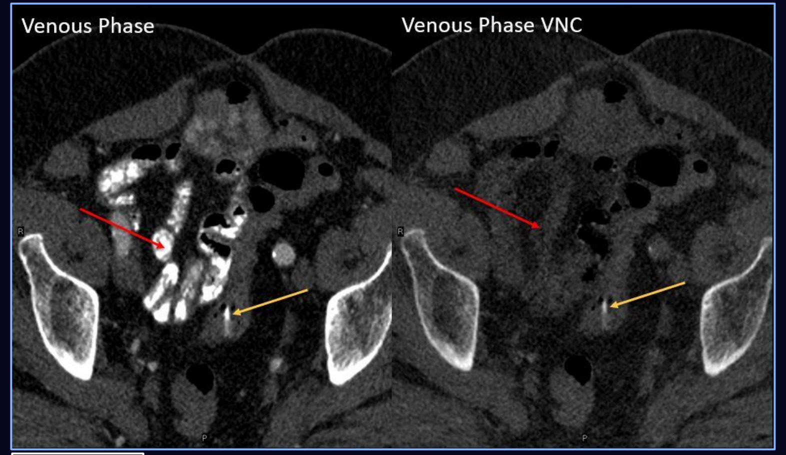

Figure 1

Effective Dose: 27.5 mSv
Table Time: 4:38 min

Figure 2

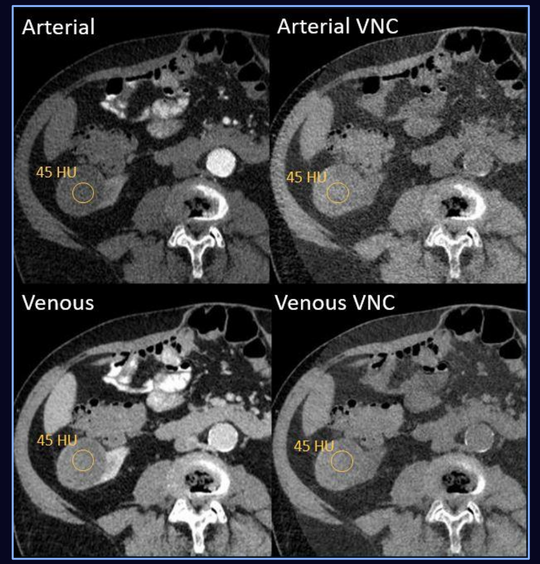

Figure 1. Dual-energy GIB CTA demonstrates how the iodine in oral contrast material (red arrows) is subtracted on the VNC images. However, the linear hyperdensity seen in the sigmoid colon (yellow arrows) remains on the VNC images, consistent with intraluminal calcific material, and NOT intraluminal hemorrhage.

Figure 2. The same exam also demonstrated a hyperdense cyst within the right kidney. The VNC images demonstrate absence of enhancement / iodine in the cyst given the unchanged HU density (yellow circles) on enhanced and VNC images.

Methods:

- We analyzed the literature to find previously described parameters for performing dual-energy CTA for GI bleeding (Wells 2018). The protocols were modified after phantom testing and approved by our departmental medical physicists for clinical use. The DE CTA protocol included only arterial and venous acquisitions with VNC reconstructions and iodine maps. All scans were performed on second or third generation dual source CT scanners (Siemens Healthineers, Erlangen, Germany).

1) Arterial Phase
2) Arterial Iodine Map
3) Arterial Phase VNC

1) Venous Phase
2) Venous Iodine Map
3) Venous Phase VNC

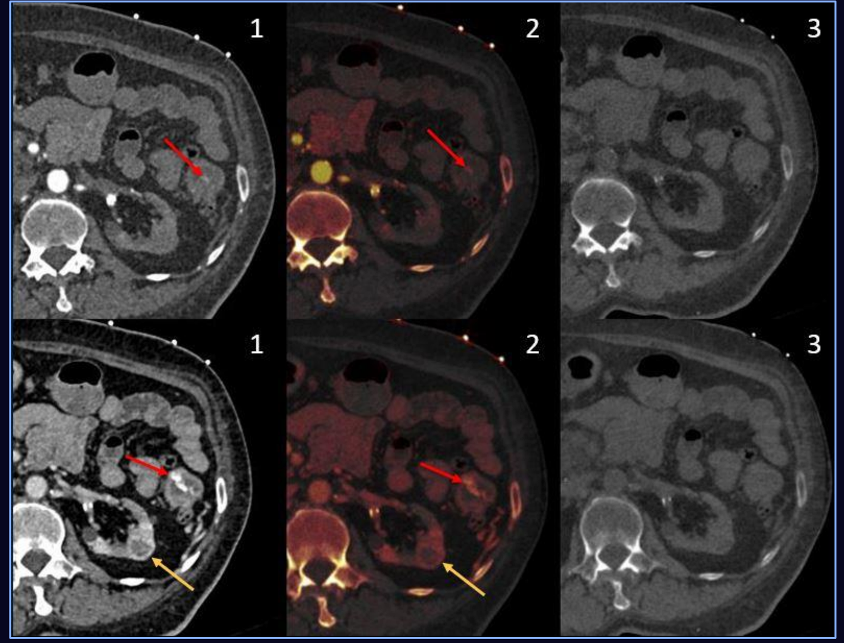

Dual-energy GIB CTA demonstrates active GI bleeding in the jejunum (red arrows), as well as an incidentally noted enhancing left renal mass (yellow arrows) concerning for renal cell carcinoma. The iodine map and subtraction of iodine on the VNC images demonstrate that this is true active extravasation into the bowel and true contrast enhancement of the left renal mass.

Effective Dose: 27.9 mSv
Table Time: 4:16 min

- Single-energy GIB CTA's from the previous 6 months were analyzed to determine effective dose and table time. A total of 68 single-energy GIB CTA's spanning from October 2018 through March 2019 were included in this group.
- Clinical use of the dual-energy GI Bleed CTA protocol began in March 2019. Effective dose and table time were recorded for these studies. As of July 2019, a total of 30 dual-energy GIB CTA's were included in this group.

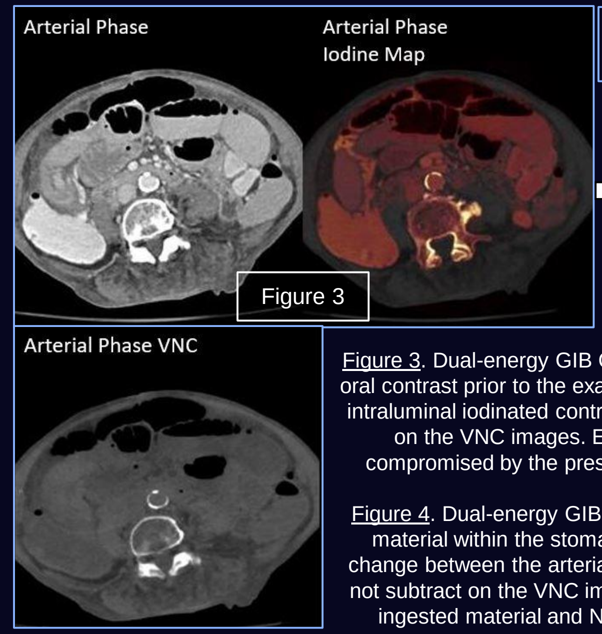

Figure 3

Effective Dose: 21.5 mSv
Table Time: 3:12 min

Effective Dose: 21.8 mSv
Table Time: 3:34 min

Figure 4

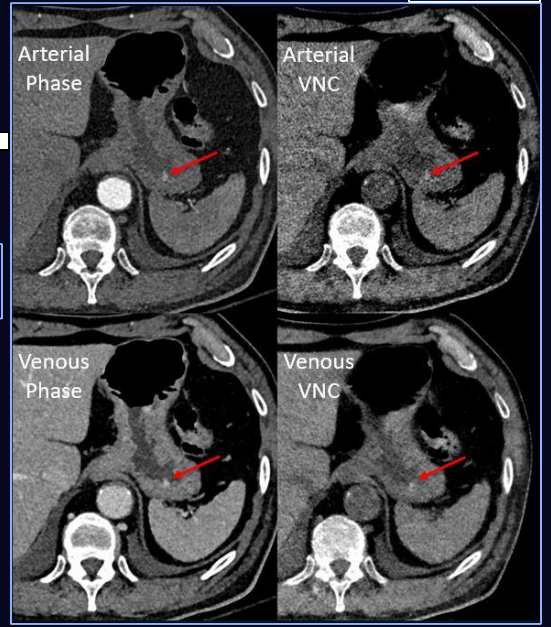

Figure 3. Dual-energy GIB CTA where the patient was given oral contrast prior to the exam. Iodine map demonstrates the intraluminal iodinated contrast material, which is subtracted on the VNC images. Evaluation for GI bleeding is compromised by the presence of oral contrast material.

Figure 4. Dual-energy GIB CTA demonstrates hyperdense material within the stomach (red arrows) that does not change between the arterial and venous phases, and does not subtract on the VNC images. This therefore represents ingested material and NOT intraluminal hemorrhage.

- Patient table time was determined by calculating the time interval from scout image to final venous image. Monte-Carlo simulation based software (Radimetrics, Bayer Healthcare) was utilized to calculate effective radiation dose. Statistical analysis was performed using log-rank test and Wilcoxon Rank Sum test.

Results:

Exam Protocol	Mean Effective Dose	Mean Table Time
Single-energy GI Bleed CTA (n=68)	38.8 mSv	4:55 minutes
Dual-energy GI Bleed CTA (n=30)	27.4 mSv	3:45 minutes

- For scans utilizing single-energy GIB CTA with three separate acquisitions, the mean effective dose was ***38.8 mSv*** and the mean table time was ***4 minutes, 55 seconds.***
- Upon implementation of the dual-energy GIB CTA protocol with two acquisitions, the mean effective dose decreased to ***27.4 mSv*** and the mean table time decreased ***to 3 minutes, 45 seconds***

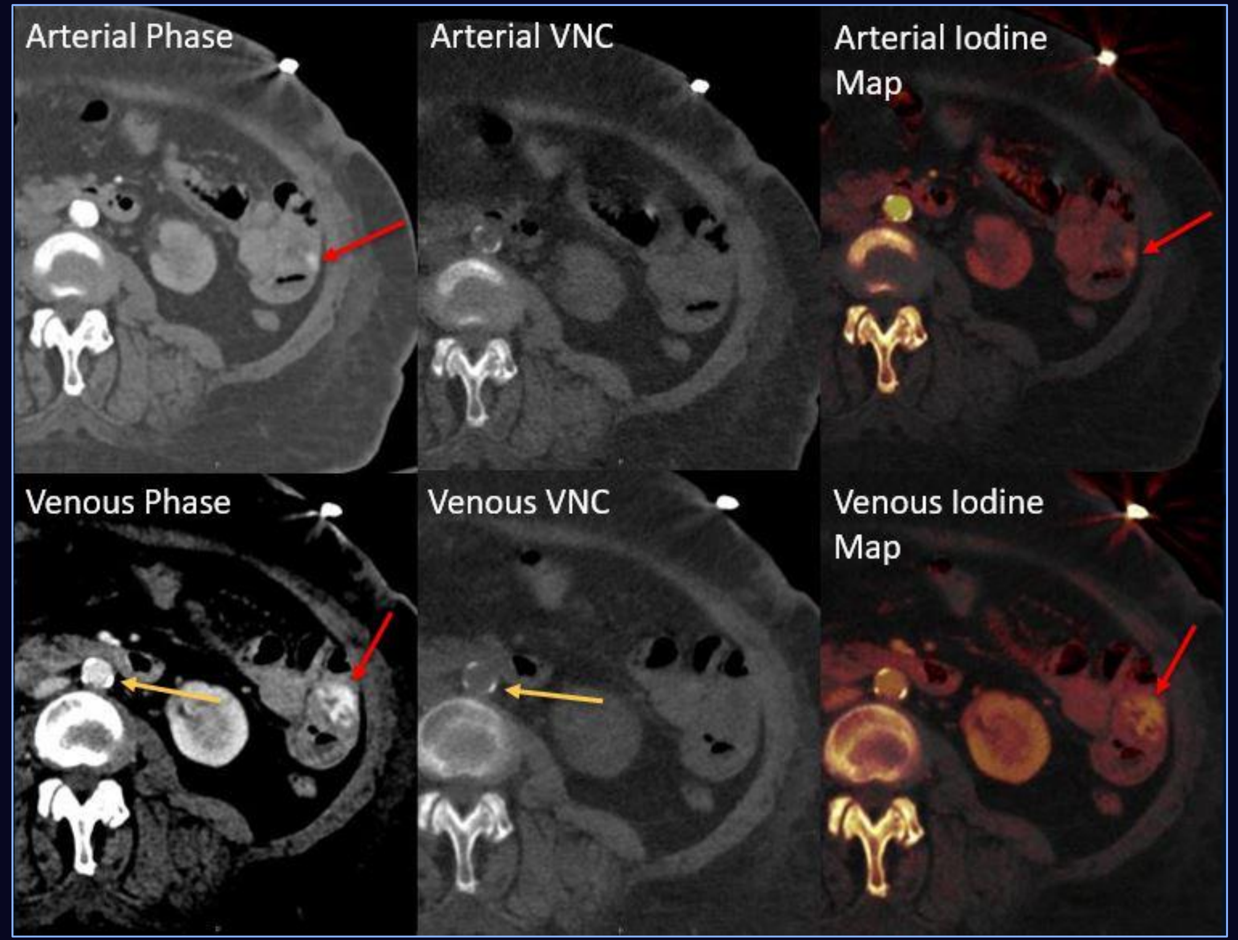

Dual-energy GIB CTA demonstrates active GI bleeding in the descending colon (red arrows). The aortic calcifications (yellow arrows) persist on the VNC images, demonstrating that only iodine is subtracted from the reconstructed non-contrast images.

Effective Dose: 22.2 mSv
Table Time: 3:54 min

- Statistical analysis demonstrated a ***significant decrease in both patient effective dose (P < 0.001) and table time (P < 0.001).***

Table 1. Summary statistics for "Total Radiation Dosage (mSv)" stratified by energy protocol

Energy Protocol	n	Mean	SD	SE	Median	P.25th	P.75th	Min	Max
Single Energy	68	38.80	14.45	1.75	37.33	28.95	51.33	13.18	70.34
Dual Energy	30	27.39	6.52	1.19	27.61	22.24	31.75	15.60	41.36

Table 2. Summary statistics for "Table Time (min)" stratified by energy protocol.

Energy Protocol	n	Mean	SD	SE	Median	P.25th	P.75th	Min	Max
Single Energy	68	4.91	1.34	0.16	4.56	3.89	5.49	3.17	8.65
Dual Energy	30	3.75	0.85	0.15	3.54	3.14	4.03	2.68	6.33

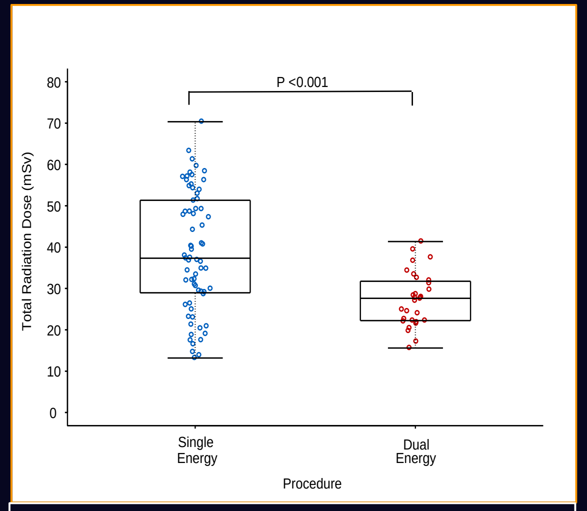

Figure 5. Empirical distributions for "Total Radiation Dose (mSv)" for the "Single Energy" and "Dual Energy" procedures. The p-value (P) was derived via the Wilcoxon Rank Sum test, in which under the null hypothesis it is assumed that the underlying median Total Radiation Dose (mSv) is the same for both procedures.

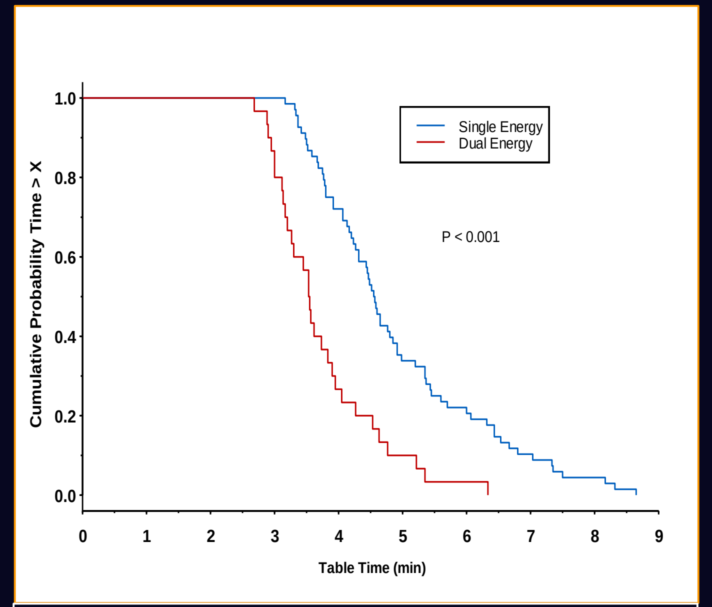

Figure 6. Empirical "Table Time (min)" cumulative distribution functions for the "Single Energy" and "Dual Energy" procedures. Note that the y-axis represents the cumulative probability that the "Table Time" was greater than the "Table Time" denoted on the x-axis. The p-value (P) was derived by way of a log-rank test, in which under the null hypothesis it is assume that the two underlying cumulative distribution function are equal.

Conclusion:

- Dual-energy CT allows significant decreases in patient radiation dose and examination time in the evaluation of GI bleeding.

- After implementation of the dual-energy GIB CTA protocol into the clinical workflow at our institution, we were able to improve the quality of patient care by maintaining the diagnostic capabilities of a three-phase GIB CTA protocol using a dual-energy GIB CTA protocol.

REFERENCES:

Artigas, J. M., Martí, M., Soto, J. A., Esteban, H., Pinilla, I., & Guillén, E. (2013). Multidetector CT angiography for acute gastrointestinal bleeding: technique and findings. Radiographics: A Review Publication of the Radiological Society of North America, Inc, 33(5), 1453–1470. https://doi.org/10.1148/rg.335125072
Bostani, M., McMillan, K., DeMarco, J. J., Cagnon, C. H., & McNitt-Gray, M. F. (2014). Validation of a Monte Carlo model used for simulating tube current modulation in computed tomography over a wide range of phantom conditions/challenges. Medical Physics, 41(11), 112101. https://doi.org/10.1118/1.4887807
Bostani, M., Mueller, J. W., McMillan, K., Cody, D. D., Cagnon, C. H., DeMarco, J. J., & McNitt-Gray, M. F. (2015). Accuracy of Monte Carlo simulations compared to in-vivo MDCT dosimetry. Medical Physics, 42(2), 1080–1086. https://doi.org/10.1118/1.4906178
Dobritz, M., Engels, H.-P., Schneider, A., Bauer, J., & Rummeny, E. J. (2009). Detection of intestinal bleeding with multi-detector row CT in an experimental setup. How many acquisitions are necessary? European Radiology, 19(12), 2862–2869. https://doi.org/10.1007/s00330-009-1510-7
García-Blázquez, V., Vicente-Bártulos, A., Olavarria-Delgado, A., Plana, M. N., van der Winden, D., Zamora, J., & EBM-Connect Collaboration. (2013). Accuracy of CT angiography in the diagnosis of acute gastrointestinal bleeding: systematic review and meta-analysis. European Radiology, 23(5), 1181–1190. https://doi.org/10.1007/s00330-012-2721-x
Gawlitza, J., Haubenreisser, H., Meyer, M., Hagelstein, C., Sudarski, S., Schoenberg, S. O., & Henzler, T. (2016). Comparison of organ-specific-radiation dose levels between 70 kVp perfusion CT and standard tri-phasic liver CT in patients with hepatocellular carcinoma using a Monte-Carlo-Simulation-based analysis platform. European Journal of Radiology Open, 3, 95–99. https://doi.org/10.1016/j.ejro.2016.04.003
Geffroy, Y., Rodallec, M. H., Boulay-Coletta, I., Jullès, M.-C., Fullès, M.-C., Ridereau-Zins, C., & Zins, M. (2011). Multidetector CT angiography in acute gastrointestinal bleeding: why, when, and how. Radiographics: A Review Publication of the Radiological Society of North America, Inc, 31(3), E35-46. https://doi.org/10.1148/rg.313105206
Kuhle, W. G., & Sheiman, R. G. (2003). Detection of active colonic hemorrhage with use of helical CT: findings in a swine model. Radiology, 228(3), 743–752. https://doi.org/10.1148/radiol.2283020756
Laine, L., Yang, H., Chang, S.-C., & Datto, C. (2012). Trends for incidence of hospitalization and death due to GI complications in the United States from 2001 to 2009. The American Journal of Gastroenterology, 107(8), 1190–1195; quiz 1196. https://doi.org/10.1038/ajg.2012.168
Machida, H., Tanaka, I., Fukui, R., Shen, Y., Ishikawa, T., Tate, E., & Ueno, E. (2016). Dual-Energy Spectral CT: Various Clinical Vascular Applications. Radiographics: A Review Publication of the Radiological Society of North America, Inc, 36(4), 1215–1232. https://doi.org/10.1148/rg.2016150185
Martí, M., Artigas, J. M., Garzón, G., Alvarez-Sala, R., & Soto, J. A. (2012). Acute lower intestinal bleeding: feasibility and diagnostic performance of CT angiography. Radiology, 262(1), 109–116. https://doi.org/10.1148/radiol.11110326
Sugi, M. D., Menias, C. O., Lubner, M. G., Bhalla, S., Mellnick, V. M., Kwon, M. H., & Katz, D. S. (2018). CT Findings of Acute Small-Bowel Entities. Radiographics: A Review Publication of the Radiological Society of North America, Inc, 38(5), 1352–1369. https://doi.org/10.1148/rg.2018170148
Wells, M. L., Hansel, S. L., Bruining, D. H., Fletcher, J. G., Froemming, A. T., Barlow, J. M., & Fidler, J. L. (2018). CT for Evaluation of Acute Gastrointestinal Bleeding. Radiographics: A Review Publication of the Radiological Society of North America, Inc, 38(4), 1089–1107. https://doi.org/10.1148/rg.2018170138
Wortman, J. R., Landman, W., Fulwadhva, U. P., Viscomi, S. G., & Sodickson, A. D. (2017). CT angiography for acute gastrointestinal bleeding: what the radiologist needs to know. The British Journal of Radiology, 90(1075), 20170076. https://doi.org/10.1259/bjr.20170076